The Effects of Admittance Term on Back-drivability

O. Işıtman[1], O. Ayit[1] and M. İ. C. Dede[1]

[1]İzmir Institute of Technology, İzmir, Turkey, e-mail: ogulcanisitman, orhanayit, candede@iyte.edu.tr

Abstract. In the design of kinesthetic haptic devices, there are two main device structures namely impedance and admittance. In a customary scenario, the human operator back-drives the haptic device by holding and providing motion to the handle of the haptic device. If the type of transmission system does not allow passive back-drivability, then the back-drivability is satisfied by the use of an admittance controller. This type of a haptic device is said to have admittance structure. The selection of the admittance term in this controller plays a critical part in the task execution performance. Determination of this term is not trivial and the optimal parameters depend on not only the key performance criteria but also on the human operator. An experimental study is carried out in this work to determine the effect of the admittance term parameters on the performance of human operators in terms of the execution of the task in minimal time and the best accuracy. In this paper, the experimental set-up and the results of the experiments are presented and discussed.

Key words: Admittance Control, Admittance Term, Back-drivability, Haptics.

1 Introduction

A typical kinesthetic haptic device acquires the motion of the targeted body part of the human operator. This information is used as the motion demand to drive the slave system in a teleoperation scenario. The physical interaction of the slave system with its environment is simultaneously measured as interaction forces/moments or if the slave system is a virtual reality scenario, then the virtual interaction forces/moments are modeled and calculated. Haptic device is used at this stage to display these forces/moments to the human operator.

In general, the targeted human body part is the hand and a handle is used to couple the human operator to the haptic device. Since the acquisition of the handle motion needs to be done at higher sampling frequencies [1] and with precision, external measurement techniques such as vision sensors or inertial measurement units cannot fulfill the task. The motion of the handle is typically calculated indirectly by using the joint sensor measurements and direct kinematics formulated for the haptic device's mechanism.

The haptic device mechanism is equipped with actuation systems in order to display forces/moments at the handle to the human. However, the human operator is required to back-drive this mechanism in order to issue motion demands for the slave system. If the actuation system is composed of customary transmission system with larger reduction ratios (typically over 1:5), then the back-drivability of the system is affected adversely if not becomes almost impossible [2]. In this situation, a passive back-drivable system otherwise named as an impedance type system should not be used. A solution is to devise an admittance type structure for active back-driving by implementing an admittance controller.

An admittance controller used in an admittance type haptic device necessitates the use of a force/moment sensor to acquire the human operator interaction with the handle. An admittance term is used to convert this interaction information to the motion demand of the haptic device, which results in back-driving the haptic mechanism. This admittance term generates a virtual coupling between the human and the handle with the components of a virtual mass-spring-damper.

The selection of these mass-spring-damper components is not a trivial process. The selection process depends on the performance criteria set for the task such as task completion duration, task accuracy or human effort during task, and the human operator's physical condition. The physical condition of the human operator can also be named as the impedance characteristics of the human arm for this specific case in which human hand motion is captured [3]. The human impedance varies from one individual to another and also it changes during the day and due to the psychological state of the same human operator [3].

In this paper an experimental study is carried out to understand the effects of the virtual coupling components and their values on the task execution performance. A single degree-of-freedom (DoF) linear system with a handle is used and a task is designed to measure the performance of various human subjects. Different admittance terms are used and the performance results in terms of positioning accuracy and the human effort are obtained and discussed.

The next section provides a brief overview of the admittance type haptic devices and their controllers. The experimental set-up and the task are explained in the following sections. The experimental results obtained are presented and discussed to conclude the paper.

2 Overview of Admittance Type Haptic Systems

In the literature, admittance type devices are rarely seen as haptic systems, however it is mandatorily used as haptic system when there are mechanical limitations such as high inertia, high friction and as a consequence of these, non-back-drivability. The admittance type haptic systems are mostly preferred in surgical operations [4, 5], rehabilitation systems [6, 7], industrial operations [8, 9] and haptic researches [10, 11].

In this type of devices, forces or torques applied from user or environment, are transformed to states of system such as position, velocity or acceleration by using admittance gain. Admittance gain is generally modeled by using combination of mass, spring and damper components. In [12] and [13], admittance gain is designed as a mass/inertia to mimic free translational/rotational motion. By that way, the measured force/torque is converted to acceleration. In addition, other states are obtained by using integral operation to derive desired values for low-level controller in the system. Another type of admittance gain model is used in a RML-glove which is a five-fingered admittance haptic interface. In this system, admittance gain is modeled as a virtual spring component for relating force to position [14]. To obtain relation between velocity and applied force, only damper component is used to design admittance gain as implemented in [15] and [16]. Also, virtual mass-damper model can be used to obtain a desired physical coupling with the environment by calculating the velocity from the measured forces as used in [17] and [18]. Furthermore, mass-spring-damper model is commonly used as an admittance gain and some works that used this model are [19] and [20]. Besides the mentioned models, E. Faulring et al. use dynamic simulation to compute desired acceleration from applied force for admittance type hand controller [21]. Also, W.Yu et al. designed a model free PID admittance controller for an Upper Limb Exoskeleton [22].

Even though mass-spring-damper compositions are mostly preferred as admittance term in literature, there are not enough studies on determination of the values of these components. In [23], an experiment is performed with the participation of 15 subjects to evaluate controllability of device. According to results of experiment, the optimum values of mass-damper components are designated for each subject separately. Moreover, M. Nambi et al. prepared an experiment to investigate different damper values as an admittance term which minimizes the force tracking error [16]. In literature, the spring parameter is mostly chosen as zero in composing the admittance term. In this paper, the effects of choosing mass – damper components with spring and without spring components are investigated in composition of the admittance term.

3 Experimental Set-up

A single degree of freedom admittance type device is used in the experiments as shown in Fig. 1. To obtain linear motion, a DC motor (HITACHI D06D401E) with an optical encoder (AEDA-3300AT) is assembled to a lead screw linear stage which has 220 mm length workspace. Since the resolution of the quadrature optical encoder is 16384 counts/rev and the lead screw stage has 5mm pitch, the linear resolution of the system is obtained as 0.03 μm. In addition to these, a handle, which forces the user to hold it in precision grasp, is mounted on the top of the linear stage to interact with the subjects. Below the handle, a Kistler (type 9017B)

3 DoF force sensor is placed. A NI MyRIO 1900 data acquisition (DAQ) systems is used for digital and analog data acquisition and controlling the system. DAQ system has a 12-bit ±10 V analog input to get force data. Also, by using the device, analog outputs are issued as demands to the Maxon 4-Q-DC servo-amplifier that is used to drive the motor. To meet the power requirements of the system, a 20 V DC power supply is used. Control algorithm and graphical user interface is developed in NI LabView Software with Control Design and Simulation module and Real-Time module. Force readings are acquired and control algorithm is executed at a sampling rate of 1 kHz.

Admittance control is implemented on top of a low-level velocity controller, which is selected to be a proportional controller (P-controller). The implemented control scheme is shown in Fig. 2. Low-level controller gain K_p is experimentally found by observing minimal tracking error for given sinusoidal velocity input. In Fig. 2, G_c represents the low-level velocity controller. F_{ref} is reference force which is selected to be zero for free motion (full back-drivability), A is admittance term, X_m is measured position, X_e is the position vector of the contacted environment, V_s and F_s are the velocity sensor transfer function and force sensor transfer function, respectively.

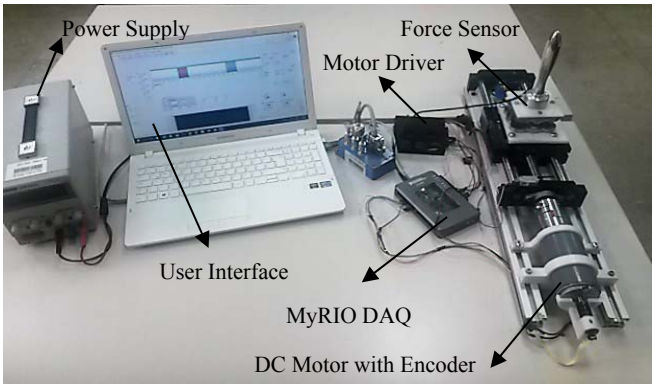

Fig 1. Experimental Set-up.

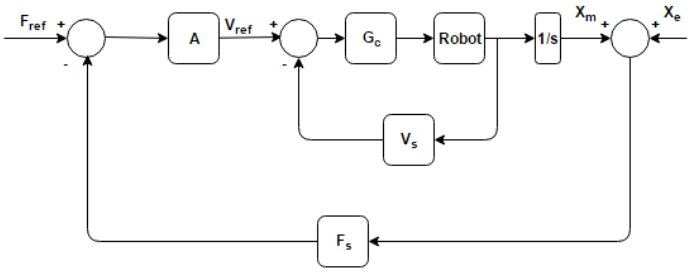

Fig. 2 Control Scheme of Single Dof Admittance Type Device.

Admittance control requires measurements of the interaction forces between the robot and its environment; as well as accurate trajectory following capabilities. Hence, this implies that a robot with high power actuators and a stiff construction is preferred, which puts specific demands on the robot's design.

In an admittance controller, a force set point is specified and it is tracked by a force compensator given in Equations 1 and 2; where F, V, m, b, k and A parameters refer to force, velocity, mass, damper, spring and admittance term, respectively. Force compensator can be modeled as a mass, spring and damper system.

$$F(s) = m.sV(s) + b.\mathrm{V}(s) + \frac{1}{s}k.V(s) \quad (1)$$

$$\frac{V(s)}{F(s)} = \frac{s}{ms^2+bs+\mathrm{k}} = A \quad (2)$$

Determination of the parameters is constructed under consideration of tracking capability limit of the set-up and feasibility for the human force limits. The experimental setup, which is described above, has a 19 rad/s (3 Hz) tracking capability as calculated by carrying out a frequency response analysis.

Characteristics of the admittance term depend on the chosen parameters. High admittance term causes sudden reaction, while low admittance term gives a slow reaction to the applied force. Although the mass and the damper coefficients which are inversely proportional to the admittance term, they are chosen as low as possible to initiate the robot motion softly. However, selecting very low values for the coefficients cause the system to be very sensitive to the interaction forces.

4 Description of the Task

To determine the effect of the admittance term parameters on the performance of human operators, an experiment is designed. A task is organized to evaluate the accuracy and the energy usage of the subjects with different parameters.

In this task, the subject is asked to hold the handle, which is designed for the subject to have a precision type of grasp, with his/her dominant hand. As guided by the graphical user interface, the subject is instructed to move handle to blue target and keep it there for four seconds as indicated by the user interface. After four seconds, the subject moves the handle to the red target and holds the handle at that location for four seconds. The subject repeats this process 2 times without releasing the handle. When the user reaches the target for the last time, it is requested to release the handle without any further action.

The visual information displayed to the human subject is shown in Fig. 3. The black bar demonstrates handle's position and targets are represented as a red (on the left) and blue (on the right) bars. The white region near the targets presents the score board which is created to define a metric for comparison between the pa-

rameters. Fig. 4 presents the score range used on both targets based on the position of the handle. When the black cursor is inside the one of the targets, the indicator in green color by default, which is represented by rectangular area above the targets, turns to red color for 4 seconds then turns back to green again. This gives the information to the user that he/she can move the handle to the other target. Since the human hand's movements may jiggle, this waiting duration provides us to obtain more reliable results about scoring the accuracy experiment.

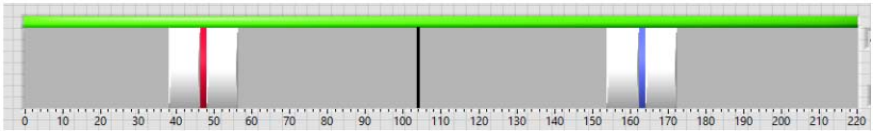

Fig 3. Graphical user interface for the generated task

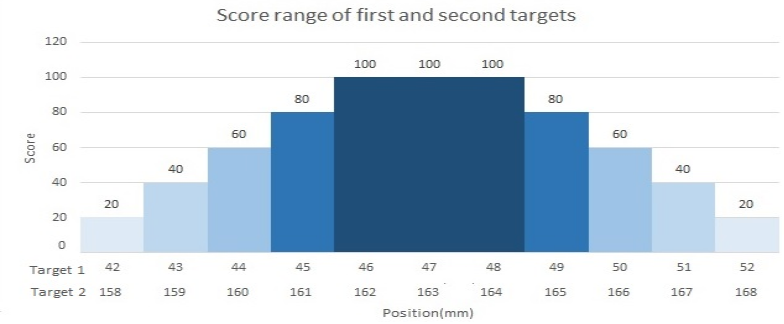

Fig 4. Score range of first target based on position

The evaluation of the effort of the subjects while moving the handle is carried out by using Equation 3 where F, x, E_{kin}, E_{damp}, E_{spr}, and E_{lost} represent force, position, kinetic energy, dissipated energy due to virtual damper, potential energy stored in the virtual spring and energy lost due to viscous friction, respectively. Since the relative results are investigated, energy loss of the system is neglected for the given equation. Also, at the end of the experiment, the handle comes back to its static condition again, for that reason sum of the kinetic energy terms is equal to zero. During the experiments for each subject and each admittance parameter tested, locations of the targets are kept the same.

$$\begin{gathered} F_1(x_1 - x_0) = E_{kin1} + E_{damp1} + E_{spr1} + E_{lost1} \\ E_{spr1} + F_2(x_2 - x_1) = E_{kin2} + E_{damp2} + E_{spr2} + E_{lost2} \\ \vdots \\ F_n(x_n - x_{n-1}) = E_{kin\,n} + E_{damp\,n} + E_{spr\,n} + E_{lost\,n} \\ E_{sprn} = E_{kin\,n+1} + E_{damp\,n+1} + E_{lost\,n+1} \end{gathered} \tag{3}$$

$$\sum_{1}^{n} F_n \Delta x_n = \sum E_{kin} + \sum E_{damp} + \sum E_{lost}$$

As it can be observed from the energy equation, potential energy of the spring term cancels out between each state. Due to these conditions, damping term dissipates all the energy in the experiments.

5 Experimental Results

The experiments are carried out with the participation of 4 women and 9 men subjects. The ages of these 13 subjects are varying between 24 and 32. Subjects are informed about the experiment and the task. Each subject is required to practice with the device before the experiment. For this practice, admittance parameters are chosen different from the inspected ones not to affect the reliability of the comparison-based results.

Each subject participated in 6 experiments, which can be grouped in two main categories. In the first group of experiments, admittance term is modeled as spring - mass - damper and in the second group, it is modeled without the spring element. Table 1 presents chosen admittance parameters and designated corner frequency against the experiment number. Damping ratio ζ of the admittance term $(\frac{K\omega_n{}^2 s}{s^2+2\zeta\omega_n s+\omega_n{}^2})$ is kept constant to determine parameters with respective to desired natural frequency ω_n.

Table 1. Mass-spring-damper parameters

Admittance Parameters				
Experiment Number	*Mass (kg)*	*Spring (N/m)*	*Damping (N.s/m)*	*Corner Frequency (rad/s)*
1	2	2	3,78	1
2	2	18	11,38	3
3	2	72	22,77	6
4	2	0	2	1
5	2	0	6	3
6	2	0	12	6

The spring parameter is adjusted to reach the desired corner frequency in first three experiments. For last three experiments, damper parameter is modified to obtain the desired corner frequencies. The value of the natural frequency for the first experiment and the value of the corner frequency for the fourth one are the same and that is 1. In the same manner between the experiments 2-5 and 3-6 these values are 3 and 6, respectively. The effect of the spring term is investigated by comparing these groups of experiments. The main reason to keep these the same is

to have similar bandwidths for two types of admittance terms with and without the spring component.

Table 2. Scores of Subjects

Accuracy						
Subject	*Exp # 1*	*Exp # 2*	*Exp # 3*	*Exp # 4*	*Exp # 5*	*Exp # 6*
1	77,28	76,80	91,23	66,67	86,85	85,47
2	88,72	93,21	90,46	71,42	78,63	90,27
3	89,75	89,02	90,32	55,91	72,67	68,25
4	92,22	93,03	94,92	68,04	79,71	80,15
5	84,51	81,59	92,85	82,36	79,41	84,41
6	80,21	87,49	90,86	67,34	84,57	87,78
7	71,59	84,43	85,90	69,60	84,68	85,47
8	61,14	88,94	90,08	51,56	82,10	74,70
9	47,03	77,82	78,19	67,50	74,71	83,84
10	62,79	89,85	85,48	58,78	69,31	75,84
11	68,25	75,32	73,98	57,78	81,69	76,58
12	72,60	90,40	90,08	67,04	76,31	84,22
13	88,30	91,25	82,74	70,31	84,03	90,81
Average	75,72	86,09	87,47	65,71	79,59	82,14

Result of the accuracy experiments is given in the Table 2 with the average values of the each set of experiments. The results can be investigated separately in each group of the experiment. With the increasing corner frequency, obtained accuracy scores also increase. Similar outcome is also observed in last three experiments. In contrast, the results between the experiment groups, which have same corner frequencies, are decreasing and that indicates the effect of spring term.

Table 3. Energy Consumption of Subjects

Energy Consumpiton (J)						
Subject	*Exp # 1*	*Exp # 2*	*Exp # 3*	*Exp # 4*	*Exp # 5*	*Exp # 6*
1	0,12	0,34	0,50	0,05	0,10	0,21
2	0,06	0,16	0,34	0,04	0,11	0,23
3	0,05	0,17	0,37	0,05	0,20	0,17
4	0,07	0,20	0,43	0,04	0,09	0,14
5	0,13	0,28	0,50	0,05	0,12	0,20
6	0,07	0,28	0,55	0,05	0,09	0,16
7	0,07	0,18	0,40	0,06	0,10	0,28
8	0,06	0,16	0,32	0,04	0,08	0,15
9	0,09	0,21	0,47	0,03	0,06	0,11
10	0,12	0,20	0,54	0,05	0,12	0,19
11	0,06	0,18	0,36	0,03	0,07	0,15
12	0,08	0,23	0,55	0,02	0,12	0,19
13	0,11	0,28	0,50	0,04	0,11	0,23
Average	0,08	0,22	0,45	0,04	0,10	0,18

The energy supplied by the user to the system in each experiment is listed in Table 3. The units for these results are in Joules. As observed in the accuracy experiments, energy consumption which indicates the effort by the user increases as the chosen corner frequency values are increased. The experiment groups which do not include spring term use less energy with respect to the first three groups.

6 Discussions and Conclusions

During the literature survey, it is observed that mass–spring–damper model is commonly used as admittance term due to the effective usage and simple design. For that reason, an experimental study is carried out to investigate the effects of mass, spring and damper component for back-drivability success. An experimental setup is prepared and a task is defined to evaluate the effects on the human operator. The results of experiments, which are evaluated in terms of accuracy and energy consumption according to the described task, are presented in Section 5. According to these results, spring term is one of the essential parameter to influence accuracy in contrast to energy consumption. In the first three experiments, the corner frequency is increased while the damping ratio is kept constant and that causes the better accuracy and higher energy consumption. This is a natural and an expected result due to the usage of higher spring coefficients to increase natural frequency, ω_n. On the other hand, increasing the corner frequency of admittance term also enhance accuracy and energy consumption as observed in last three experiment which have mass-damper model. In addition to these, increasing the coefficients of admittance term requires higher force values and it is limited with the operating limits of the user. Consistency of outcome can be supported by inspecting the energy consumption results. By interpreting the obtained results, mass – spring – damper parameters can be chosen optimal for specific tasks. For the tasks that require accuracy, the higher spring coefficient in the admittance term must be preferred such as in surgical robots. In contrast to that, the spring parameter might be unnecessary for rehabilitation tasks due to high-energy consumption.

Acknowledgements

This work is supported in part by The Scientific and Technological Research Council of Turkey via grant number 115E726.

References

1. Kern, Thorsten A., ed. Engineering haptic devices: a beginner's guide for engineers. Springer Science & Business Media, 2009 pp. 56-58.
2. Ishida, Tatsuzo, and Atsuo Takanishi. "A robot actuator development with high backdrivability." 2006 IEEE Conference on Robotics, Automation and Mechatronics. IEEE, 2006.
3. Podobnik, Janez. Haptics for virtual reality and teleoperation. Vol. 64. Springer Science & Business Media, 2012 pp. 52-54.
4. Osa, Takayuki, et al. "Hybrid Rate—Admittance Control With Force Reflection for Safe Teleoperated Surgery." IEEE/ASME Transactions on Mechatronics 20.5 (2015): 2379-2390.
5. Melo, Javier, Emilio Sánchez, and Iñaki Díaz. "Adaptive admittance control to generate real-time assistive fixtures for a COBOT in transpedicular fixation surgery." 2012 4th IEEE RAS & EMBS Int. Conference on Biomedical Robotics and Biomechatronics. IEEE, 2012.
6. Ozkul, Fatih, and Duygun Erol Barkana. "Design of an admittance control with inner robust position control for a robot-assisted rehabilitation system RehabRoby." Advanced Intelligent Mechatronics (AIM), 2011 IEEE/ASME International Conference on. IEEE, 2011.
7. Kooren, Peter N., et al. "Design and control of the Active A-Gear: A wearable 5 DOF arm exoskeleton for adults with Duchenne muscular dystrophy." Biomedical Robotics and Biomechatronics (BioRob), 2016 6th IEEE International Conference on. IEEE, 2016.
8. Tang, Te, et al. "Teach industrial robots peg-hole-insertion by human demonstration." Advanced Intelligent Mechatronics (AIM), 2016 IEEE Int. Conference on. IEEE, 2016.
9. Clover, C. L., et al. "Dynamic simulation of virtual mechanisms with haptic feedback using industrial robotics equipment." Robotics and Automation, 1997. Proceedings., 1997 IEEE International Conference on. Vol. 1. IEEE, 1997.
10. Parthiban, Chembian, and Michael R. Zinn. "A simplified approach to admittance-type haptic device impedance evaluation." 2014 IEEE Haptics Symposium (HAPTICS). IEEE, 2014.
11. Wang, Hongbo, and Kazuhiro Kosuge. "Control of a robot dancer for enhancing haptic human-robot interaction in waltz." IEEE transactions on haptics 5.3 (2012): 264-273.
12. Peer, Angelika, and Martin Buss. "A new admittance-type haptic interface for bimanual manipulations." IEEE/ASME Transactions on mechatronics 13.4 (2008): 416-428.
13. Morbi, A., and Mojtaba A. "Safely Rendering Small Impedances in Admittance-Controlled Haptic Devices." IEEE/ASME Transactions on Mechatronics 21.3 (2016): 1272-1280.
14. Ma, Zhou, and Pinhas Ben-Tzvi. "An Admittance Type Haptic Device: RML Glove." ASME 2011 International Mechanical Engineering Congress and Exposition. American Society of Mechanical Engineers, 2011.
15. Arbuckle, Troy K., et al. "Human Velocity Control of Admittance-Type Robotic Devices With Scaled Visual Feedback of Device Motion." IEEE Transactions on Human-Machine Systems 46.6 (2016): 859-868.
16. Manikantan, N., Provancher, W. R., Abbott, J. J. "On the ability of humans to apply controlled forces to admittance-type devices." Advanced Robotics 25.5 (2011): 629-650.
17. Bortole, M., et al. "A robotic exoskeleton for overground gait rehabilitation." Robotics and Automation (ICRA), 2013 IEEE International Conference on. IEEE, 2013.
18. Heidingsfeld, M., et al. "A force-controlled human-assistive robot for laparoscopic surgery." 2014 IEEE Int. Conference on Systems, Man, and Cybernetics (SMC). IEEE, 2014.
19. Nabeel, Muhammad, et al. "Increasing the impedance range of admittance-type haptic interfaces by using Time Domain Passivity Approach." Intelligent Robots and Systems (IROS), 2015 IEEE/RSJ International Conference on. IEEE, 2015.
20. Baumeyer, Julien, et al. "Robotic co-manipulation with 6 DoF admittance control: Application to patient positioning in proton-therapy." 2015 IEEE International Workshop on Advanced Robotics and its Social Impacts (ARSO). IEEE, 2015.

21. Faulring, Eric L., J. Edward Colgate, and Michael A. Peshkin. "The cobotic hand controller: design, control and performance of a novel haptic display." The International Journal of Robotics Research 25.11 (2006): 1099-1119.
22. Yu, Wen, Jacob Rosen, and Xiaoou Li. "PID admittance control for an upper limb exoskeleton." Proceedings of the 2011 American Control Conference. IEEE, 2011.
23. Ozkul F., Barkana Erol D., "Bir Robot Destekli Rehabilitasyon Sisteminin Admitans Filtre Parametrelerinin Adaptif Olarak Ayarlanması", Otomatik Kontrol Ulusal Toplantısı TOK, Eskişehir, 29 Eylül-1 Ekim 2016.